TRANSACTIONS ON EMERGING TELECOMMUNICATIONS TECHNOLOGIES
Trans. Emerging Tel. Tech. 2015; **26**:918–928
Published online 30 November 2013 in Wiley Online Library (wileyonlinelibrary.com). DOI: 10.1002/ett.2764

RESEARCH ARTICLE

Space–time block code design for LTE-advanced systems

Van-Bien Pham*

Faculty of Radio-Electronics, Le Quy Don Technical University, Vietnam

ABSTRACT

The number of time slot (or symbols per slot in 3rd Generation Partnership Project language) in the long-term evolution frame structure for data transmission is not guaranteed to be an even number, so the Alamouti orthogonal space–time block code (STBC) can not be applied. Recently, Lei *et al.* (*Institute of Electrical and Electronics Engineers Transactions on Wireless Communications, 2011*) introduced a quasi-orthogonal space time block code (QOSTBC) for two transmit antennas and three time slots (which is named as L-QOSTBC in this paper). This code achieves two desirable properties as full rate and full diversity. However, the main disadvantage of the L-QOSTBC is high decoding complexity due to pair-symbol maximum likelihood decoding. In this paper, we propose a novel three-time-slot STBC (TTS-STBC) for two transmit antennas. The proposed TTS-STBC can achieve full-rate full-diversity transmission with single-symbol maximum likelihood decoding. In comparison to L-QOSTBC, the proposed TTS-STBC has lower decoding complexity and higher coding gain. In addition, a new decoding strategy for the proposed TTS-STBC that named as single-symbol quasi-maximum likelihood is also developed to overcome the performance degradation caused by time-varying fading channels. Simulation results show that the proposed TTS-STBC outperforms the L-QOSTBC in both quasi-static and time-varying fading channels. Copyright © 2013 John Wiley & Sons, Ltd.

***Correspondence**
Van-Bien Pham, Faculty of Radio-Electronics, Le Quy Don Technical University, Vietnam.
E-mail: phamvanbien@mta.edu.vn

Received 17 May 2013; Revised 11 October 2013; Accepted 21 October 2013

1. INTRODUCTION

Recently, the 3rd Generation Partnership Project (3GPP), which standardised long-term evolution (LTE), has been deployed worldwide to provide an access rate of up to 100 Mbps. The 3GPP is now working on the next generation wireless system (fourth generation—4G) under the project LTE-advanced, building upon the legacy standard LTE release 8 [1]. It is known that user equipment (i.e. mobile station) will support a minimum of two antennas to achieve spatial diversity [2]. For this case, the well-known Alamouti code [3] would be the most suitable candidate for uplink transmission. Unfortunately, it has been revealed that the LTE frame structure does not always contain an even number of time slots, and thus direct application of the Alamouti code is inappropriate. This unfortunate observation initiates an interesting space–time block code (STBC) design problem for a system with three time slots and two transmit antennas. As in the case of the Alamouti code, the desired STBC should achieve full-rate and full-diversity transmission with low decoding complexity. However, to the best of our knowledge, there is no such STBC available at present.

In [4], a hybrid scheme of STBC for three time slots was proposed by repeating one more time slot after the Alamouti STBC (called H-STBC code in this thesis). The H-STBC code achieves relatively good performance and requires only single-symbol maximum likelihood (SML) decoding at the receiver. However, the H-STBC code does not allow for achieving full diversity. In a latest study [5], Lei *et. al*. introduced a QOSTBC code for three time slots and two transmit antennas (called L-QOSTBC code in this paper) using pair-symbol maximum likelihood (PML) decoding. The L-QOSTBC code achieves full-rate and full-diversity, but it has low coding gain and high decoding complexity. High complexity is also a problem when the L-QOSTBC code uses PML decoder rather than SML decoder.

In this paper, we design STBC for three time slots and two-antenna transmission (abbreviated as TTS-STBC code). The proposed TTS-STBC code achieves full-rate and full-diversity transmission while requiring low decoding complexity with the SML decoder. The proposed TTS-STBC code is thus superior to both the H-STBC code and the TTS-QOSTBC code in terms of error performance and also to the TTS-QOSTBC code in terms of decoding complexity. Furthermore, by exploiting the orthogonal combining technique in [6] and [7], we develop a low complexity single-symbol quasi-maximum likelihood (SQML) decoding method for the proposed TTS-STBC code to overcome the performance degradation caused by time-varying fading channels. The proposed SQML decoding method can more effectively remove the inter-transmit antenna interference induced by time-varying fading channels than the SML decoding method without increasing computational complexity. A part of this framework has been illustrated in our previous work [8].

This paper is organised as follows. The system model and LTE-advanced frame structure are presented in Section 2. An overview of the H-STBC code and the L-QOSTBC code for LTE-advanced is presented in Section 3. The proposed TTS-STBC code and its properties are provided in Section 4. Low complexity decoders for the proposed TTS-STBC code are presented in Section 5. Some numerical results as well as performance comparisons are provided in Section 6. Section 7 presents some related work and discussions. Finally, conclusions are presented in Section 7.

2. THE SYSTEM MODEL AND LTE-ADVANCED FRAME STRUCTURE

2.1. The system model

We consider an LTE-advance uplink model where the transmitter (i.e. mobile station) is equipped with two antennas and the receiver (i.e. base station - BS) is equipped with N_R antennas as illustrated in Figure 1.

At each time slot t, signals x_t and y_t are transmitted simultaneously from antennas 1 and 2, respectively. The random path gains are $\boldsymbol{h}_m(t) = \begin{bmatrix} h_{1m}(t) & h_{2m}(t) \end{bmatrix}^T$ $(m = 1, \ldots, N_R)$, where $h_{1m}(t)$ and $h_{2m}(t)$ correspond to the gains from the transmit antennas 1 and 2, respectively, to the receive antenna m at t time slot. At the receiver, the signal received by antenna m at time t is given by

$$r_{tm} = h_{1m}(t)x_t + h_{2m}(t)y_t + n_{tm} \tag{1}$$

where n_{tm} are the samples of independent complex random Gaussian noise on the m^{th} antenna with zero-mean. Assuming perfect channel knowledge, the receiver computes the maximum likelihood decision statistics

$$\sum_{t=1}^{L}\sum_{m=1}^{N_R} |r_{tm} - h_{1m}(t)\, x_t - h_{2m}(t) y_t|^2 \tag{2}$$

over all possible codewords $x_1 y_1 x_2 y_2 \ldots x_L y_L$ to decide in favour of codeword minimising (2).

2.2. LTE-ADVANCED FRAME STRUCTURE

Figure 2 illustrates the radio frame of uplink transmission in LTE-advanced systems, which is presented in [5]. Each radio frame is 10 ms long with 10 sub-frames or 20 transmission units. Here, the transmission unit refers to the term 'slot' in 3GPP. We use the term 'transmission unit' to avoid confusion of the 'slot' concept in STBC. Each transmission unit lasts 0.5 ms consisting of either seven symbols in the normal cyclic-prefix mode or six symbols in the extended cyclic-prefix mode. One or two of the six or seven symbols per transmission unit will be taken up by demodulation reference signal and sounding reference signal as shown in the figure (illustrated by shaded symbols). The remaining symbols will be used for data transmission. From the figure, it can be seen that each transmission unit always, be it in the normal cyclic-prefix mode or the extended cyclic-prefix mode, contains an odd number of (three symbols) time duration (or 'slot' in STBC context).

3. OVERVIEW OF THE H-STBC CODE AND THE L-QOSTBC CODE

3.1. The H-STBC code

Alamouti code is designed for two transmission slots for wireless systems equipped with two transmit antennas. Unfortunately, they are not applicable to the systems with time slot restrictions as described in the previous texts. When the number of time slots is restricted to three, as in the LTE-advanced frame, there are two options for encoding the three transmit symbols (denote the three symbols to be transmitted as s_1, s_2 and s_3). The first option is to use the full-rate alternative H-STBC code [4], and the second

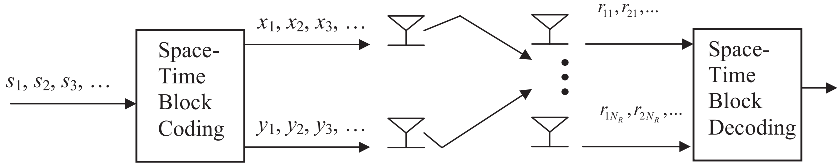

Figure 1. The space-time block code system model with two transmit antennas.

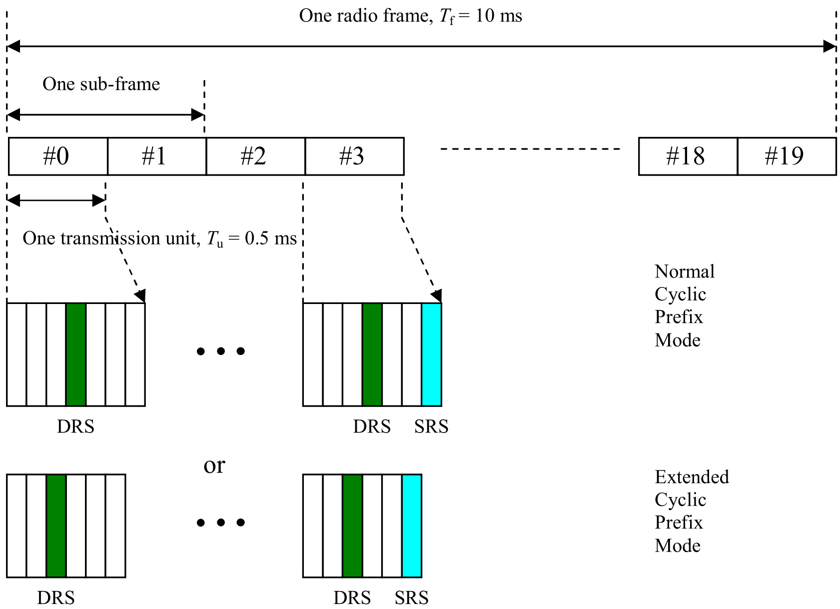

Figure 2. Frame structure of long-term evolution-advanced uplink.

option is to use the L-QOSTBC code [5]. The encoding matrix for the H-STBC code is given by

$$\boldsymbol{S}_{\mathrm{H}} = \begin{bmatrix} s_1 & s_2^* \\ s_2 & -s_1^* \\ s_3 & s_3 \end{bmatrix} \tag{3}$$

where two columns represent symbols transmitted from two transmit antennas while the rows indicate transmit symbols at three time slots. The encoding scheme is simple as the first two time slots are still encoded as in the orthogonal Alamouti code, while the third time slot is simply repeated from two antennas. This simple encoding scheme allows for linear decoding with low complexity at the receiver. However, it is clear that the scheme is not able to provide full-diversity gain as spatial diversity is not achieved in the third time slot. As a result, it suffers from significant performance loss as compared to the orthogonal Alamouti code.

3.2. The L-QOSTBC code

In order to achieve full diversity gain for the case with three time slots and two transmit antennas, the L-QOSTBC was proposed by Lei *et. al.* [5]. Codeword matrix of the L-QOSTBC is given by

$$\boldsymbol{S}_{\text{L-QOSTBC}} = \begin{bmatrix} s_1 & y_1 \\ s_2 & y_2 \\ s_3 & y_3 \end{bmatrix} \tag{4}$$

where the data symbols y_1, y_2, and y_3 are linear combinations of the transmitted symbols s_1, s_2, and s_3 on the 1st antenna, which can be represented mathematically as

$$\begin{bmatrix} y_1 & y_2 & y_3 \end{bmatrix}^{\mathrm{T}} = \boldsymbol{A} \begin{bmatrix} s_1^* & s_2^* & s_3^* \end{bmatrix}^T \tag{5}$$

and

$$\boldsymbol{A} = \begin{bmatrix} a_{11} & a_{12} & a_{13} \\ a_{21} & a_{22} & a_{23} \\ a_{31} & a_{32} & a_{33} \end{bmatrix} = \frac{1}{3} \begin{bmatrix} 1 & 2e^{j\frac{2\pi}{5}} & 2e^{-j\frac{2\pi}{5}} \\ -2e^{j\frac{2\pi}{5}} & e^{-j\frac{\pi}{5}} & 2 \\ -2e^{-j\frac{2\pi}{5}} & 2 & e^{j\frac{\pi}{5}} \end{bmatrix} \triangleq \begin{bmatrix} \boldsymbol{b}_1 \\ \boldsymbol{b}_2 \\ \boldsymbol{b}_3 \end{bmatrix} \tag{6}$$

From (6) and (1), the received signal can be rewritten as

$$\boldsymbol{r} = \boldsymbol{H} \begin{bmatrix} \boldsymbol{s} \\ \boldsymbol{s}^* \end{bmatrix} + \boldsymbol{n} \tag{7}$$

where $\boldsymbol{s} = (s_1, s_2, s_3)^{\mathrm{T}}$, $\boldsymbol{r} = (\boldsymbol{r}_1, \boldsymbol{r}_2, \ldots, \boldsymbol{r}_{N_R})^{\mathrm{T}}$ with $\boldsymbol{r}_m = (r_{1m}, r_{2m}, r_{3m})^{\mathrm{T}}$, $\boldsymbol{n} = (\boldsymbol{n}_1, \boldsymbol{n}_2, \ldots, \boldsymbol{n}_{N_R})^{\mathrm{T}}$ with $\boldsymbol{n}_m = (n_{1m}, n_{2m}, n_{3m})^T$ are the transmitted signals, received signals and noise, respectively, in three symbol times. $\boldsymbol{H} = [\boldsymbol{H}_1, \boldsymbol{H}_2, \ldots, \boldsymbol{H}_{N_R}]^{\mathrm{T}}$ is the $3N_{\mathrm{R}} \times 6$ equivalent channel matrix, where

$$\boldsymbol{H}_m = \begin{bmatrix} h_{1m}(1) & 0 & 0 & h_{2m}(1)\,\boldsymbol{b}_1 \\ 0 & h_{1m}(2) & 0 & h_{2m}(2)\,\boldsymbol{b}_2 \\ 0 & 0 & h_{1m}(3) & h_{2m}(3)\,\boldsymbol{b}_3 \end{bmatrix} \tag{8}$$

When the channel is quasi-static fading, that is, $h_{1m}(t) = h_{1m}, h_{2m}(t) = h_{2m}, t = 1, 2, 3$ then

$$\boldsymbol{H}_m = \begin{bmatrix} h_{1m}\boldsymbol{I}_3 & h_{2m}\boldsymbol{A} \end{bmatrix} \tag{9}$$

Trans. Emerging Tel. Tech. **26**:918–928 (2015) © 2013 John Wiley & Sons, Ltd.
DOI: 10.1002/ett

where $\boldsymbol{I}_3$ is the three-dimensional identity matrix. To decode $\boldsymbol{s}$ from the received signal $\boldsymbol{r}$, we augment the received signal vector (7) with its conjugate $\boldsymbol{r}^*$ as

$$\bar{\boldsymbol{r}} = \bar{\boldsymbol{H}} \begin{bmatrix} \boldsymbol{s} \\ \boldsymbol{s}^* \end{bmatrix} + \bar{\boldsymbol{n}} \tag{10}$$

where

$$\begin{aligned} \bar{\boldsymbol{r}} &= \begin{bmatrix} \boldsymbol{r}_1 & \boldsymbol{r}_1^* & \boldsymbol{r}_2 & \boldsymbol{r}_2^* & \dots & \boldsymbol{r}_{N_R} & \boldsymbol{r}_{N_R}^* \end{bmatrix}^T, \\ \boldsymbol{n} &= \begin{bmatrix} \boldsymbol{n}_1 & \boldsymbol{n}_1^* & \boldsymbol{n}_2 & \boldsymbol{n}_2^* & \dots & \boldsymbol{n}_{N_R} & \boldsymbol{n}_{N_R}^* \end{bmatrix}^T \end{aligned} \tag{11}$$

$$\bar{\boldsymbol{H}} = [\bar{\boldsymbol{H}}_1, \bar{\boldsymbol{H}}_2, \dots, \bar{\boldsymbol{H}}_{N_R}]^T, \ \bar{\boldsymbol{H}}_m = \begin{bmatrix} h_{1m}\boldsymbol{I}_3 & h_{2m}\boldsymbol{A} \\ h_{2m}^*\boldsymbol{A}^* & h_{1m}^*\boldsymbol{I}_3 \end{bmatrix} \tag{12}$$

Using the specially designed $\boldsymbol{A}$ in (6), decoding three elements in $\boldsymbol{s}$ can be decoupled into decoding one element and decoding two elements separately without losing diversity order through linear processing. We multiply the sufficient statistics $\bar{\boldsymbol{H}}^H$ to both sides of the Equation (10),

$$\tilde{\boldsymbol{r}} = \bar{\boldsymbol{H}}^H \bar{\boldsymbol{r}} = \bar{\boldsymbol{H}}^H \bar{\boldsymbol{H}} \begin{bmatrix} \boldsymbol{s} \\ \boldsymbol{s}^* \end{bmatrix} + \bar{\boldsymbol{H}}^H \bar{\boldsymbol{n}} \tag{13}$$

where $\tilde{\boldsymbol{r}} = \left(\tilde{\boldsymbol{r}}_1, \tilde{\boldsymbol{r}}_2, \dots, \tilde{\boldsymbol{r}}_{N_R}\right)^T$ with

$$\begin{aligned} \tilde{\boldsymbol{r}}_m &= \left(\tilde{r}_{6(m-1)+1}, \tilde{r}_{6(m-1)+2}, \dots, \tilde{r}_{6(m-1)+6}\right)^T \\ &\triangleq \left(r'_{1m}, r'_{2m}, \dots, r'_{6m}\right)^T \end{aligned} \tag{14}$$

$$\boldsymbol{G}_{2m} = \begin{bmatrix} |h_{1m}|^2 + |h_{2m}|^2 & 0 & 2a_{22}h_{1m}^*h_{2m} & h_{1m}^*h_{2m}(a_{23}+a_{32}) \\ 0 & |h_{1m}|^2 + |h_{2m}|^2 & h_{1m}^*h_{2m}(a_{23}+a_{32}) & 2a_{33}h_{1m}^*h_{2m} \\ 2a_{22}^*h_{1m}h_{2m}^* & h_{1m}h_{2m}^*(a_{23}+a_{32}) & |h_{1m}|^2 + |h_{2m}|^2 & 0 \\ h_{1m}h_{2m}^*(a_{23}+a_{32}) & 2a_{33}^*h_{1m}h_{2m}^* & 0 & |h_{1m}|^2 + |h_{2m}|^2 \end{bmatrix}; m = 1, \dots, N_R \tag{26}$$

and

$$\bar{\boldsymbol{H}}^H \bar{\boldsymbol{H}} = \begin{bmatrix} \bar{\boldsymbol{H}}_1^H \bar{\boldsymbol{H}}_1 & \bar{\boldsymbol{H}}_2^H \bar{\boldsymbol{H}}_2 & \dots & \bar{\boldsymbol{H}}_{N_R}^H \bar{\boldsymbol{H}}_{N_R} \end{bmatrix}^T \tag{15}$$

where

$$\bar{\boldsymbol{H}}_m^H \bar{\boldsymbol{H}}_m = \begin{bmatrix} |h_{1m}|^2 \boldsymbol{I}_3 + |h_{2m}|^2 \boldsymbol{A}^T \boldsymbol{A}^* & h_{1m}^* h_{2m} (\boldsymbol{A} + \boldsymbol{A}^T) \\ h_{1m} h_{2m}^* (\boldsymbol{A}^* + \boldsymbol{A}^H) & |h_{1m}|^2 \boldsymbol{I}_3 + |h_{2m}|^2 \boldsymbol{A}^H \boldsymbol{A} \end{bmatrix} \tag{16}$$

Therefore, the linear Equation (13) can be used to decode $\boldsymbol{s}$. In fact, because of the specially designed $\boldsymbol{A}$ in (6), we have

$$\boldsymbol{A}^H \boldsymbol{A} = \boldsymbol{A}^T \boldsymbol{A}^* = \boldsymbol{I}_3 \tag{17}$$

$$\boldsymbol{A} + \boldsymbol{A}^T = \left(\boldsymbol{A}^* + \boldsymbol{A}^H\right)^* = \begin{bmatrix} 2a_{11} & 0 & 0 \\ 0 & 2a_{22} & a_{23}+a_{32} \\ 0 & a_{23}+a_{32} & 2a_{33} \end{bmatrix} \tag{18}$$

With (17) and (18), (13) can be 'broken' into two sub-equations without any performance loss as opposed to ML detection as

$$\hat{\boldsymbol{r}}_1 = \bar{\boldsymbol{G}}_1 \begin{bmatrix} s_1 & s_1^* \end{bmatrix}^T + \hat{\boldsymbol{n}}_1 \tag{19}$$

$$\hat{\boldsymbol{r}}_1 = \begin{bmatrix} r'_{11} & r'_{41} & \dots & r'_{1N_R} & r'_{4N_R} \end{bmatrix}^T \tag{20}$$

$$\bar{\boldsymbol{G}}_1 = \begin{bmatrix} \boldsymbol{G}_{11} & \boldsymbol{G}_{12} & \dots & \boldsymbol{G}_{1N_R} \end{bmatrix}^T \tag{21}$$

$$\begin{aligned} \boldsymbol{G}_{1m} = &\begin{bmatrix} |h_{1m}|^2 + |h_{2m}|^2 & 2a_{11}h_{1m}^*h_{2m} \\ 2a_{11}^*h_{1m}h_{2m}^* & |h_{1m}|^2 + |h_{2m}|^2 \end{bmatrix}; \\ &m = 1, \dots, N_R \end{aligned} \tag{22}$$

And

$$\hat{\boldsymbol{r}}_2 = \bar{\boldsymbol{G}}_2 \begin{bmatrix} s_2 & s_3 & s_2^* & s_3^* \end{bmatrix}^T + \hat{\boldsymbol{n}}_2 \tag{23}$$

$$\hat{\boldsymbol{r}}_2 = \begin{bmatrix} r'_{21} & r'_{31} & r'_{51} & r'_{61} & \dots & r'_{2N_R} & r'_{3N_R} & r'_{5N_R} & r'_{6N_R} \end{bmatrix}^T \tag{24}$$

$$\bar{\boldsymbol{G}}_2 = \begin{bmatrix} \boldsymbol{G}_{21} & \boldsymbol{G}_{22} & \dots & \boldsymbol{G}_{2N_R} \end{bmatrix}^T \tag{25}$$

Therefore, the optimal ML decoding metric (2) of received signal (10) can be expanded as a sum of two items,

$$\left| \bar{\boldsymbol{r}} - \bar{\boldsymbol{H}} \begin{bmatrix} \boldsymbol{s} & \boldsymbol{s}^* \end{bmatrix}^T \right|^2 = f_1(s_1) + f_{23}(s_2, s_3) \tag{27}$$

where

$$f_1(s_1) = \left| \hat{\boldsymbol{r}}_1 - \bar{\boldsymbol{G}}_1 \begin{bmatrix} s_1 & s_1^* \end{bmatrix}^T \right|^2 \tag{28}$$

$$f_{23}(s_2, s_3) = \left| \hat{\boldsymbol{r}}_2 - \bar{\boldsymbol{G}}_2 \begin{bmatrix} s_2 & s_3 & s_2^* & s_3^* \end{bmatrix}^T \right|^2 \tag{29}$$

Because $f_{23}(s_2, s_3)$ is a function of two symbols, this decoding method is called a PML decoding method.

In comparison to the H-STBC code, the L-QOSTBC code achieves full-rate and full-diversity gain with improved bit-error-rate (BER) performance. However, because the L-QOSTBC code uses PML decoding rather than SML decoding, its complexity is still quite high.

Moreover, although the L-QOSTBC code can achieve full diversity gain, there is still an amount of signal-to-noise ratio (SNR) loss because of not maximising coding gain [5].

In the next section, we will design a new TTS-STBC code, which can simultaneously achieve four desirable properties, namely full-rate, full-diversity gain, high coding gain and low decoding complexity.

4. THE PROPOSED TTS-STBC AND ITS PROPERTIES

4.1. Code construction

The encoder starts with an input symbol vector $\boldsymbol{s} = [s_1, s_2, s_3]^T$ of three information symbols chosen from a square quadrature amplitude modulation (QAM) constellation A, where $s_k = s_{kI} + \mathbf{j}s_{kQ}$ with s_{kI} and s_{kQ} denoting the in-phase and quardrature part of the complex symbol s_k, respectively. The proposed TTS-STBC code is constructed in the following three steps.

- *Step 1*: Rotating the input symbol vector $\boldsymbol{s}$ to generate the rotated symbol vector $\boldsymbol{x} = \boldsymbol{s}e^{\mathbf{j}\theta}$. This is equivalent to rotating constellation A and choosing symbol x_k from the rotated constellation $\mathrm{A}e^{\mathbf{j}\theta}$. The purpose of the constellation rotation is to ensure full diversity and maximum coding gain.
- *Step 2*: Coordinating interleaved elements of vector $\boldsymbol{x}$ to generate vector $\boldsymbol{u} = [u_1\, u_2\, u_3]^T$ based on the following interleaving rules: $u_1 = x_{1\mathrm{I}} + \mathbf{j}x_{3\mathrm{Q}}, u_2 = x_2, u_3 = x_{3\mathrm{I}} + \mathbf{j}x_{1\mathrm{Q}}$.
- *Step 3*: Encoding u_k according to the following encoding matrix

$$\boldsymbol{S} = \begin{bmatrix} u_1 & -u_2^* & u_3 \\ u_2 & u_1^* & u_3 \end{bmatrix}^{\mathrm{T}} \tag{30}$$

Clearly, the proposed encoding scheme transmits three symbols in three time slots, so it achieves a rate of one. Moreover, the transmit symbols from the two antennas have the same average power, that is, $\mathrm{E}\left[|u_1|^2\right] = \mathrm{E}\left[|u_2|^2\right] = \mathrm{E}\left[|u_3|^2\right]$. This means that our proposed code minimises the signal power fluctuation on the transmitter side.

4.2. Full diversity and maximal coding gain

In order to meet the full-diversity criterion, the codeword difference matrix $\boldsymbol{B} = \boldsymbol{S} - \boldsymbol{S}'$ should be of full-rank (i.e. rank 2), or equivalently,

$$\det(\boldsymbol{B}^{\mathrm{H}}\boldsymbol{B}) = \det\begin{bmatrix} \sum_{k=1}^{3}\left|u_k - u'_k\right|^2 & \left|u_3 - u'_3\right|^2 \\ \left|u_3 - u'_3\right|^2 & \sum_{k=1}^{3}\left|u_k - u'_k\right|^2 \end{bmatrix} \neq 0 \tag{31}$$

where $\boldsymbol{S}$ and $\boldsymbol{S}'$ are two distinct codeword matrices obtained from (30). In order to prove this fact, we must first show that the minimum determinant $\delta_{\min} = \min\{\det(\boldsymbol{B}^H\boldsymbol{B})\}$ is a non-zero for any distinct codeword pairs $\boldsymbol{S}$ and $\boldsymbol{S}'$ of the proposed TTS-STBC code. Let $\Delta x_{k\mathrm{I}} = x_{k\mathrm{I}} - x'_{k\mathrm{I}}$ and $\Delta x_{k\mathrm{Q}} = x_{k\mathrm{Q}} - x'_{k\mathrm{Q}}; k = 1, 2, 3$, denote the differences in real and imaginary parts of the transmitted and erroneously detected information symbols x_k and x'_k, respectively, for any $x_k, x_k' \in \mathrm{A}e^{\mathbf{j}\theta}$ and $x_k \neq x'_k$. We calculate the value $\delta_{\min}$ of the proposed TTS-STBC code as follows:

$$\delta_{\min} = \min\left\{ \begin{array}{l} \left[(\Delta x_{1\mathrm{I}})^2 + (\Delta x_{2\mathrm{I}})^2 + (\Delta x_{2\mathrm{Q}})^2 + (\Delta x_{3\mathrm{Q}})^2\right] \\ \times\left[(\Delta x_{1\mathrm{I}})^2 + 2(\Delta x_{1\mathrm{Q}})^2 + (\Delta x_{2\mathrm{I}})^2 + (\Delta x_{2\mathrm{Q}})^2 + 2(\Delta x_{3\mathrm{I}})^2 + (\Delta x_{3\mathrm{Q}})^2\right] \end{array} \right\} \tag{32}$$

It is obvious that (32) takes its minimum value when only one information symbol is erroneous. We have three cases as follows:

- *Case 1*: If the erroneous symbol is x_1 (i.e. $x_1 \neq x'_1$), then the resulting minimum determinant is given by

$$\delta_{\min,1} = \min\left\{(\Delta x_{1\mathrm{I}})^2\left[(\Delta x_{1\mathrm{I}})^2 + 2\left(\Delta x_{1\mathrm{Q}}\right)^2\right]\right\} \tag{33}$$

- *Case 2*: If the erroneous symbol is x_2 (i.e. $x_2 \neq x'_2$), then the minimum determinant is

$$\delta_{\min,2} = \min\left\{\left[(\Delta x_{2\mathrm{I}})^2 + \left(\Delta x_{2\mathrm{Q}}\right)^2\right]^2\right\} \tag{34}$$

- *Case 3*: If the erroneous symbol is x_3 (i.e. $x_3 \neq x_3$'), then we have the resulting minimum determinant

$$\delta_{\min,3} = \min\left\{\left(\Delta x_{3\mathrm{Q}}\right)^2\left[2\left(\Delta x_{3\mathrm{I}}\right)^2 + \left(\Delta_{3\mathrm{Q}}\right)^2\right]\right\} \tag{35}$$

It is clear that the $\delta_{\min,2}$ value is a nonzero for any constellation A, the $\delta_{\min,1}$ value is a nonzero with only constellation A where $\Delta x_{k\mathrm{I}} = x_{k\mathrm{I}} - x'_{k\mathrm{I}} \neq 0$ ($x_k, x'_k \in$ A and $x_k \neq x'_k$) and the $\delta_{\min,3}$ value is a nonzero with only constellation A where $\Delta x_{k\mathrm{Q}} = x_{k\mathrm{Q}} - x'_{k\mathrm{Q}} \neq 0$. Thus, the value $\delta_{\min}$ in (10) is a nonzero if and only if the information symbol x_k is taken from constellation A where $\Delta x_{k\mathrm{I}}\Delta x_{k\mathrm{Q}} \neq 0$.

From the aforementioned observations, we can see that the proposed TTS-STBC code cannot achieve full-diversity if the information symbol x_k takes value from the conventional signal constellations A like the regular M-ary QAM or symmetric M-ary phase-shift keying (PSK). However, by rotating the constellation in *Step 1*

Trans. Emerging Tel. Tech. **26**:918–928 (2015) © 2013 John Wiley & Sons, Ltd.
DOI: 10.1002/ett

(Section 4.1), we can ensure $\Delta x_{kI}\Delta x_{kQ} \neq 0 \left(\forall x_k, x'_k \in \mathrm{A}e^{j\theta} \text{ and } x_k \neq x'_k\right)$ for any square M-ary QAM or symmetric M-ary PSK constellation A, that is, it ensures a nonzero $\delta_{\min}$ value. This means that the proposed TTS-STBC can achieve full-diversity. After having shown the full-diversity property, we have to choose the optimum constellation rotation (CR) angle to maximise the $\delta_{\min}$ value for the proposed TTS-STBC code to achieve maximum coding gain. It is not difficult to demonstrate that $\delta_{\min,2}$ is always greater or equal to $\delta_{\min,1}$ and $\delta_{\min,3}$. Thus, the optimum CR angle is chosen to maximise value of function in the succeeding texts

$$\mathrm{F} = \max\min(\max\delta_{\min,1}, \max\delta_{\min,3}) \tag{36}$$

The analytical derivation of the optimum CR angle is unfortunately not as tractable; hence, we rely on a computer search to find the optimum CR angle for the proposed TTS-STBC. For 4-QAM constellation A where signal points are $s = (2n-3)+\mathbf{j}(2m-3)$ with $n, m \in [1,2]$, as shown in Figure 3, the optimum CR angle is found to be 31.0 degrees.

5. LOW COMPLEXITY DECODERS FOR THE PROPOSED TTS-STBC CODE

5.1. Single-symbol maximum likelihood decoder

From code structure (30) and the equivalent channel model given in (19), the received signal can be represented in matrix form by

$$\boldsymbol{r} = \mathbf{H}\,\boldsymbol{u} + \boldsymbol{n} \tag{37}$$

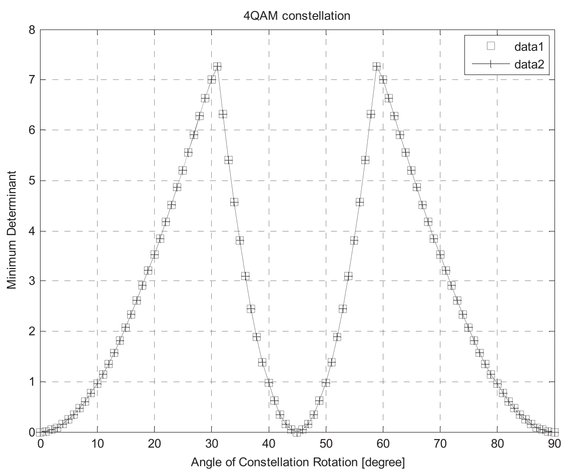

Figure 3. Optimization of 4-quadrature amplitude modulation rotation angle for the proposed three-time-slot space-time block code; data 1 and data 2 represent, respectively, values of $\delta_{\min,1}$ and $\delta_{\min,3}$.

where $\boldsymbol{u} = (u_1, u_2, u_3)^T$, $\boldsymbol{r} = \left(\boldsymbol{r}_1, \boldsymbol{r}_2, \ldots, \boldsymbol{r}_{N_R}\right)^T$ with $\boldsymbol{r}_m = (r_{1m}, r_{2m}, r_{3m})^T$, and $\boldsymbol{n} = (\boldsymbol{n}_1, \boldsymbol{n}_2, \ldots, \boldsymbol{n}_{N_R})^T$ with $\boldsymbol{n}_m = (n_{1m}, n_{2m}, n_{3m})^T$ are the transmitted signals, received signals and noise, respectively, in three symbol time. $\mathbf{H} = \left[\mathrm{H}_1^{\mathrm{T}}, \mathrm{H}_2^{\mathrm{T}}, \ldots, \mathrm{H}_{N_\mathrm{R}}^{\mathrm{T}}\right]^{\mathrm{T}}$ is the $3N_R \times 3$ equivalent channel matrix, where

$$\mathrm{H}_m = \begin{bmatrix} h_{1m}(1) & h_{2m}(1) & 0 \\ h_{2m}^*(2) & -h_{1m}^*(2) & 0 \\ 0 & 0 & h_{1m}(3) + h_{2m}(3) \end{bmatrix} \tag{38}$$

We multiply the sufficient statistics $\mathbf{H}^{\mathrm{H}}$ to both sides of the Equation (38)

$$\underbrace{\begin{bmatrix} \bar{r}_1 \\ \bar{r}_2 \\ \bar{r}_3 \end{bmatrix}}_{\bar{\boldsymbol{r}}=\mathbf{H}^{\mathrm{H}}\boldsymbol{r}} = \underbrace{\begin{bmatrix} \alpha_1 & \varepsilon & 0 \\ \varepsilon^* & \alpha_2 & 0 \\ 0 & 0 & \beta \end{bmatrix}}_{\boldsymbol{G}=\mathbf{H}^{\mathrm{H}}\mathbf{H}} \underbrace{\begin{bmatrix} u_1 \\ u_2 \\ u_3 \end{bmatrix}}_{\boldsymbol{u}} + \underbrace{\begin{bmatrix} \bar{n}_1 \\ \bar{n}_2 \\ \bar{n}_3 \end{bmatrix}}_{\bar{\boldsymbol{n}}=\mathbf{H}^{\mathrm{H}}\boldsymbol{n}} \tag{39}$$

where

$$\begin{aligned} \alpha_1 &= \sum_{m=1}^{N_R} \left(|h_{1m}(1)|^2 + |h_{2m}(2)|^2\right); \\ \alpha_2 &= \sum_{m=1}^{N_R} \left(|h_{1m}(2)|^2 + |h_{2m}(1)|^2\right) \end{aligned} \tag{40}$$

$$\begin{aligned} \beta_1 &= \sum_{m=1}^{N_R} |h_{1m}(3) + h_{2m}(3)|^2; \\ \varepsilon &= \sum_{m=1}^{N_R} \left(h_{1m}^*(1)\,h_{2m}(1) - h_{1m}^*(2)h_{2m}(2)\right) \end{aligned} \tag{41}$$

When the channel is quasi-static, $\mathbf{H}$ is orthogonal (i.e. the Grammian matrix $\boldsymbol{G}$ is diagonal) with $\alpha_1 = \alpha_2 = \alpha$ and $\varepsilon = 0$. Then, by separating and rearranging the in-phase and quadrature-phase components of $\bar{r}_1$ and $\bar{r}_3$, we have the following SML decision metrics

$$\hat{x}_1 = \arg\min_{\hat{x}\in\mathrm{A}e^{j\theta}} \left\{\beta\left|\bar{r}_{1\mathrm{I}} - \alpha\hat{x}_\mathrm{I}\right|^2 + \alpha\left|\bar{r}_{3\mathrm{Q}} - \beta\hat{x}_\mathrm{Q}\right|^2\right\} \tag{42}$$

$$\hat{x}_2 = \arg\min_{\hat{x}\in\mathrm{A}e^{j\theta}} \left\{\left|\bar{r}_2 - \alpha\hat{x}\right|^2\right\} \tag{43}$$

$$\hat{x}_3 = \arg\min_{\hat{x}\in\mathrm{A}e^{j\theta}} \left\{\alpha\left|\bar{r}_{3\mathrm{I}} - \beta\hat{x}_\mathrm{I}\right|^2 + \beta\left|\bar{r}_{1\mathrm{Q}} - \alpha\hat{x}_\mathrm{Q}\right|^2\right\} \tag{44}$$

5.2. Single-symbol quasi-maximum likelihood decoder

When the quasi-static channel conditions are not satisfied (i.e. the channel is time-varying), the effective channel matrix $\mathbf{H}$ is no longer orthogonal and the off-diagonal term ε is not zero, which introduces interference between consecutive symbols. Thus, the above SML decoder suffers from performance degradation. This motivates the need for effective decoding techniques that work well in time-varying fading. Based on the decoding method presented in [6, 7], which is originally for the Alamouti code and coordinate-interleaving orthogonal designs over time-varying fading channels, we propose an SQML decoder to overcome the detrimental effect of the time-selectivity of fading channels for the proposed TTS-STBC code as follows. First, we introduce a simple matrix transformation for orthogonal combining as

$$\bar{\boldsymbol{A}} = \begin{bmatrix} -a_{22} & a_{12} \\ a_{21} & -a_{11} \end{bmatrix} \quad \text{for} \quad \boldsymbol{A} = \begin{bmatrix} a_{11} & a_{12} \\ a_{21} & a_{22} \end{bmatrix} \tag{45}$$

Then, by combining $\boldsymbol{r}$ in (37) by $\bar{\mathbf{H}} = \left[\bar{\mathbf{H}}_1, \bar{\mathbf{H}}_2, \ldots, \bar{\mathbf{H}}_{N_R}\right]$ with the sub-matrices

$$\bar{\mathbf{H}}_m = \begin{bmatrix} h_{1m}^*(2) & h_{2m}(1) & 0 \\ h_{2m}^*(2) & -h_{1m}(1) & 0 \\ 0 & 0 & h_{1m}^*(3) + h_{2m}^*(3) \end{bmatrix}; \quad m = 1, 2, \ldots, N_R \tag{46}$$

we obtain

$$\underbrace{\bar{\mathbf{H}}\boldsymbol{r}}_{\bar{\boldsymbol{y}}} = \underbrace{\bar{\mathbf{H}}\,\mathbf{H}}_{\bar{\boldsymbol{G}}}\, u + \underbrace{\bar{\mathbf{H}}\boldsymbol{n}}_{\boldsymbol{v}} \tag{47}$$

$$\Rightarrow \begin{bmatrix} \bar{y}_1 \\ \bar{y}_2 \\ \bar{y}_3 \end{bmatrix} = \begin{bmatrix} g_1 & 0 & 0 \\ 0 & g_1 & 0 \\ 0 & 0 & g_2 \end{bmatrix} \begin{bmatrix} u_1 \\ u_2 \\ u_3 \end{bmatrix} + \begin{bmatrix} v_1 \\ v_2 \\ v_3 \end{bmatrix} \tag{48}$$

where

$$\begin{aligned} g_1 &= \sum\nolimits_{m=1}^{N_R} \left(h_{1m}^*(2) h_{1m}(1) + h_{2m}^*(2) h_{2m}(1)\right); \\ g_2 &= \sum\nolimits_{m=1}^{N_R} \left(|h_{1m}(3) + h_{1m}(3)|^2\right) \end{aligned} \tag{49}$$

By multiplying both sides in Equation (47) by $\bar{\boldsymbol{G}}^{\mathrm{H}}$, we obtain

$$\underbrace{\bar{\boldsymbol{G}}^{\mathrm{H}}\bar{\boldsymbol{y}}}_{\hat{\boldsymbol{y}}} = \underbrace{\bar{\boldsymbol{G}}^{\mathrm{H}}\bar{\boldsymbol{G}}}_{\boldsymbol{D}}\, \boldsymbol{u} + \underbrace{\bar{\boldsymbol{G}}^{\mathrm{H}}\boldsymbol{v}}_{\bar{\boldsymbol{v}}} \tag{50}$$

$$\Rightarrow \begin{bmatrix} \hat{y}_1 \\ \hat{y}_2 \\ \hat{y}_3 \end{bmatrix} = \begin{bmatrix} |g_1|^2 & 0 & 0 \\ 0 & |g_1|^2 & 0 \\ 0 & 0 & |g_2|^2 \end{bmatrix} \begin{bmatrix} u_1 \\ u_2 \\ u_3 \end{bmatrix} + \begin{bmatrix} \bar{v}_1 \\ \bar{v}_2 \\ \bar{v}_3 \end{bmatrix} \tag{51}$$

where

$$\begin{aligned} &\bar{v}_1 \sim \mathrm{CN}\left(0,\ |g_1|^2 \lambda_1 N_0\right); \quad \bar{v}_2 \sim \mathrm{CN}\left(0,\ |g_1|^2 \lambda_2 N_0\right); \\ &\bar{v}_3 \sim \mathrm{CN}\left(0,\ |g_2|^2 \lambda_3 N_0\right) \end{aligned} \tag{52}$$

$$\begin{aligned} \lambda_1 &= \sum\nolimits_{m=1}^{N_R} \left(|h_{1m}(2)|^2 + |h_{2m}(1)|^2\right); \\ \lambda_2 &= \sum\nolimits_{m=1}^{N_R} \left(|h_{1m}(1)|^2 + |h_{2m}(2)|^2\right); \\ \lambda_3 &= \sum\nolimits_{m=1}^{N_R} \left(|h_{1m}(3)|^2 + |h_{2m}(3)|^2\right) \end{aligned} \tag{53}$$

From (51) we can see that orthogonality can be achieved without interference terms at the cost of increasing the variance of noise terms in $\bar{\boldsymbol{v}}$. After pre-whitening noise and de-interleaving, we obtain

$$\tilde{y}_1 = \frac{\hat{y}_{1\mathrm{I}}}{|g_1|\sqrt{\lambda_1}} + \frac{\hat{y}_{3\mathrm{Q}}}{|g_2|\sqrt{\lambda_3}} = \frac{|g_1|}{\sqrt{\lambda_1}} x_{1\mathrm{I}} + \frac{|g_2|}{\sqrt{\lambda_3}} x_{1\mathrm{Q}} + \tilde{v}_1 \tag{54}$$

$$\tilde{y}_2 = \frac{\hat{y}_2}{|g_1|\sqrt{\lambda_2}} = \frac{|g_1|}{\sqrt{\lambda_2}} x_2 + \tilde{v}_2 \tag{55}$$

$$\tilde{y}_3 = \frac{\hat{y}_{3\mathrm{I}}}{|g_2|\sqrt{\lambda_3}} + \frac{\hat{y}_{1\mathrm{Q}}}{|g_1|\sqrt{\lambda_1}} = \frac{|g_2|}{\sqrt{\lambda_3}} x_{3\mathrm{I}} + \frac{|g_1|}{\sqrt{\lambda_1}} x_{3\mathrm{Q}} + \tilde{v}_3 \tag{56}$$

Finally, we obtain the following SQML decision metrics

$$\hat{x}_1 = \arg\min_{\hat{x} \in \mathrm{A}e^{j\theta}} \left\{ \left| \tilde{y}_{1\mathrm{I}} - \frac{|g_1|}{\sqrt{\lambda_1}} \hat{x}_{\mathrm{I}} \right|^2 + \left| \tilde{y}_{1\mathrm{Q}} - \frac{|g_2|}{\sqrt{\lambda_3}} \hat{x}_{\mathrm{Q}} \right|^2 \right\} \tag{57}$$

$$\hat{x}_2 = \arg\min_{\hat{x} \in \mathrm{A}e^{j\theta}} \left\{ \left| \tilde{y}_2 - \frac{|g_1|}{\sqrt{\lambda_2}} \hat{x} \right|^2 \right\} \tag{58}$$

$$\hat{x}_3 = \arg\min_{\hat{x} \in \mathrm{A}e^{j\theta}} \left\{ \left| \tilde{y}_{3\mathrm{I}} - \frac{|g_2|}{\sqrt{\lambda_3}} \hat{x}_{\mathrm{I}} \right|^2 + \left| \tilde{y}_{3\mathrm{Q}} - \frac{|g_1|}{\sqrt{\lambda_1}} \hat{x}_{\mathrm{Q}} \right|^2 \right\} \tag{59}$$

6. COMPARISON RESULTS

6.1. Comparison of decoding complexity

In this section, we compare the computational decoding complexity of the proposed TTS-STBC code with SML detection and SQML detection and the decoding complexity of the L-QOSTBC code [5] with PML detection. Analogous to [9], the overall complexity is measured in terms of the number of operations required to decode the transmitted signals for each codeword period. Using the same notation as in [9], a complex multiplication is equivalent to four real multiplications C_M and two real additions C_A, while a complex addition is equivalent to two real additions. Complexities of a square root and a real division are the same and equivalent to one real multiplication C_M. We split the complexity formula into two parts in order to represent C_M and C_A independently. We denote the complexity of the proposed TTS-STBC code by $C_{TTS,SML}$ and $C_{TTS,SQML}$ for SML detection and

Trans. Emerging Tel. Tech. **26**:918–928 (2015) © 2013 John Wiley & Sons, Ltd.
DOI: 10.1002/ett

Table I. Computational complexity of the L-QOSTBC code and the proposed three-time-slot space-time block code with $N_R = 1$ and different M modulation orders.

Modulation order $-M$			**4**	**8**	**16**	**32**	**64**	**128**	**256**
C_M	L-QOSTBC [5]	PML	2408	5984	21536	83360	329888	1314464	5249696
	Proposed TTS-STBC	SML	168	240	384	672	1248	2400	4704
		SQML	188	236	332	524	908	1676	3212
C_M	L-QOSTBC [5]	PML	1284	5364	19356	74988	296844	1182924	4725456
	Proposed TTS-STBC	SML	110	146	218	362	650	1226	2378
		SQML	134	170	242	386	674	1250	2402

TTS-STBC, three-time-slot space-time block code; SQML, single-symbol quasi-maximum likelihood; SML, single-symbol maximum likelihood.

Table II. Comparison of decoding time (*sec*) of the proposed three-time-slot space-time block code with L-QOSTBC code.

Modulation order M		**4**	**8**	**16**	**32**	**64**	**128**	**256**
L-QOSTBC [5]	ML	0.5702	1.0709	2.5941	8.0859	29.1201	112.2731	446.0485
Proposed TTS-STBC	SML	0.2895	0.3751	0.4793	0.6286	0.7762	1.0332	1.3931
	SQML	0.3190	0.3688	0.4776	0.6198	0.7681	1.0212	1.3806

TTS-STBC, three-time-slot space-time block code; ML, maximum likelihood; SML, single-symbol maximum likelihood; SQML, single-symbol quasi-maximum likelihood.

SQML detection, respectively. We also denote the complexity of the L-QOSTBC code with PML detection by $C_{Q,PML}$. If we present $C_{TTS,SML}$, $C_{TTS,SQML}$, and $C_{Q,PML}$ as two-dimensional vectors where the first dimension is the number of real multiplications and the second the number of real additions, then

$$C_{Q,PML} = N_R \left\{ \left(72M^2 + 21M + 588\right) C_A, \left(80M^2 + 24M + 672\right) C_M \right\} \tag{60}$$

$$C_{TTS,SML} = N_R \{(9M + 74)C_A, (18M + 96)C_M\} \tag{61}$$

$$C_{TTS,SQML} = N_R \{(9M + 98)C_A, (12M + 140)C_M\} \tag{62}$$

where M is the size of constellation A (e.g. M-QAM and M-PSK).

From Equations (60), (61) and (62), we can see that the decoding complexity of SML and SQML decoders for the TTS-STBC code is linearly proportional to the constellation size M and the decoding complexity of the SQML decoder is equivalent to that of the SML decoder. In contrast, the decoding complexity of PML decoder for the L-QOSTBC code is a two-order function of M^2, so the decoding complexity of the L-QOSTBC code is higher than that of the proposed TTS-STBC code. In Table I, we give a more clearly comparison between $C_{TTS,SML}$, $C_{TTS,SQML}$, and $C_{Q,PML}$ in terms of the number of real multiplications and real additions considering $N_R = 1$ for different M constellation sizes.

Moreover, to demonstrate the preciseness of the aforementioned derived decoding complexities for each STBC code, we calculate decoding time of the L-QOSTBC code and the proposed TTS-STBC code by computer simulation. The computer used for simulation has a dual-core Pentium CPU E3500 with a clock rate of 2.60 GHz and 3.2 Gb random-access memory. Decoding time was recorded for transmitted 333 codewords where information symbols taken from 4, 8, 16, 32, 64, 128 and 256-QAM constellations. The simulation results in Table II show that our proposed TTS-STBC code is more efficient than the L-QOSTBC code in terms of decoding complexity, especially for high-order modulations. These simulation results are entirely consistent with the computational results in Table I. This confirms that the proposed TTS-STBC code achieves a significant advantage over the L-QOSTBC code [5] regarding decoding complexity.

6.2. Comparison of performance

Table III shows the comparisons of rate R, diversity order G_d and coding gain G_c between the H-STBC code [4], the L-QOSTBC code [5], and the proposed TTS-STBC code.

Table III. Comparison of performance between the H-STBC code, Alamouti code, the L-QOSTBC code and the proposed three-time-slot space-time block code.

			G_c	
Code	R	G_d	4-QAM	16-QAM
H-STBC code [4]	1	N_R	0	0
Alamouti code [3]	1	$2N_R$	2.0	0.4
L-QOSTBC [5]	1	$2N_R$	0.2768	0.0554
Proposed TTS-STBC	1	$2N_R$	1.3483	0.2184

QAM, quadrature amplitude modulation; TTS-STBC, three-time-slot space-time block code.

From Table III, we can see that all three codes have the same rate, but only the L-QOSTBC code and the proposed TTS-STBC code achieve full diversity while the H-STBC code achieves partial diversity. In addition, the coding gain of the proposed TTS-STBC code is larger than that of the L-QSTBC code. Therefore, performance of the TTS-STBC code is better than that of L-QOSTBC code, as shown in Figure 4. In Figure 4, we provide simulation results of the STBC codes for two transmit antennas and one receive antenna on a quasi-static flat fading channel. The SML decoder is used for the Alamouti code, the H-STBC code and the proposed TTS-STBC code, while PML decoder is used for the TTS-QOSTBC code. The transmitted symbols were 4-QAM modulated.

From Figure 4, we can observe that the simulated BER curves of the Alamouti code, the L-QOSTBC code and the TTS-STBC code all have the same slope. This means that these codes have the same diversity order. On the other hand, the proposed TTS-STBC code outperforms the H-STBC code [4] as a result of full-diversity, especially at high SNR, for example, an SNR gain of 4 dB at BER of 10^{-3}. In comparison to the L-QOSTBC code [5], the proposed TTS-STBC code not only has lower decoding complexity due to SML decoding but also has a performance gain of 1.5 dB at BER of 10^{-3}. This is explained as follows. Although both the proposed TTS-STBC code and the L-QOSTBC code have the same transmit diversity order (order of 2), the proposed TTS-STBC code achieves larger coding gain than the L-QOSTBC code, as shown in Table III. This is due to the fact that the TTS-QOSTBC code focuses on diversity gain and thus its coding gain is not optimised [5]. Therefore, the proposed TTS-STBC code outperforms the L-QOSTBC code. In comparison to the Alamouti code, the performance gap between the proposed TTS-STBC code and the Alamouti code is due to the fact that the Alamouti code is an orthogonal design with a higher coding gain. However, the Alamouti code cannot apply for three-slot transmission.

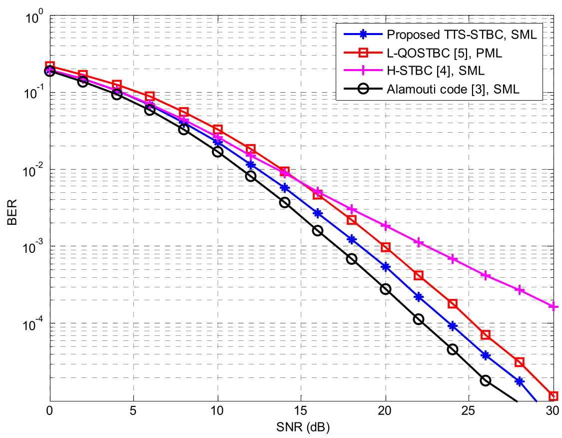

Figure 4. Performance comparisons for three-slot transmissions in quasi-static fading channel.

In Figure 5, we compare performance of the L-QOSTBC code [5] and the proposed TTS-STBC code over a time-varying fading channel. We can approximate the time-varying fading channel variation with the following autoregressive process of order 1 according to

$$h_{nl}(t+1) = \psi h_{nl}(t) + \sqrt{1-\psi^2} w_{nl}(t+1) \qquad (63)$$

where $\psi = \mathrm{E}\left[h^*_{nl}(t)h_{nl}(t+1)\right]$ denotes the fading correlation coefficient and $w_{nl}(t)$ are independent identically distributed circularly symmetric complex Gaussian random variables with zero-mean and unit variance, which are uncorrelated to $h_{nl}(t)$ [6]. The parameter $0 \leqslant \psi \leqslant 1$ characterises the degree of channel time-variations, depending on the Doppler frequency, which is caused by

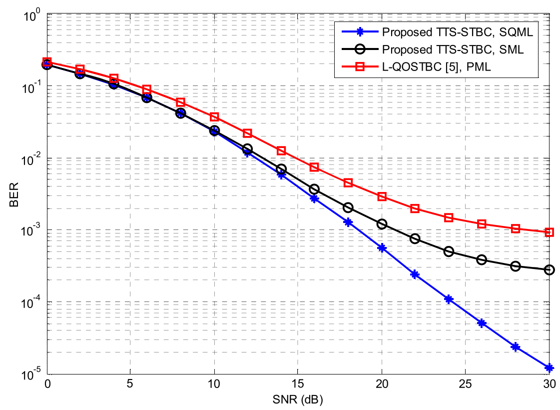

Figure 5. Performance comparison between the proposed three-time-slot space-time block code and the L-QOSTBC [5] in time-selective fading channel with the fading correlation coefficient $\psi = 0.9911$. $N_R = 1$ and 4-quadrature amplitude modulation.

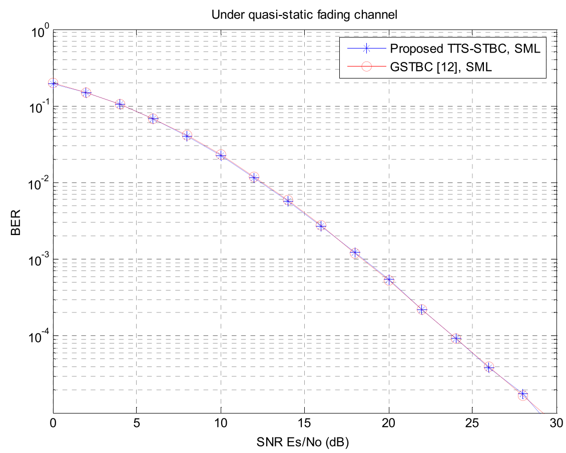

Figure 6. Performance comparisons between the proposed three-time-slot space-time block code and the group-decodable STBC [12] in quasi-static fading channel, $N_R = 1$ and 4-quadrature amplitude modulation.

Trans. Emerging Tel. Tech. **26**:918–928 (2015) © 2013 John Wiley & Sons, Ltd.
DOI: 10.1002/ett

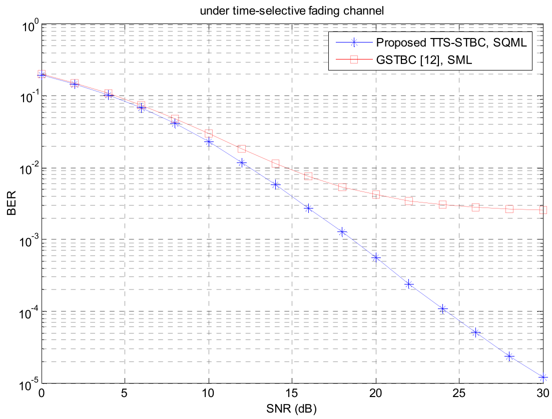

Figure 7. Performance comparisons between the proposed three-time-slot space-time block code and the group-decodable space time block code [12] in time-selective fading channel with the fading correlation coefficient $\psi = 0.9911$. $N_R = 1$ and 4-quadrature amplitude modulation.

Table IV. Comparison of peak-to-average power ratio between the proposed three-time-slot space-time block code and group-decodable space time block code [12].

Modulation	4-QAM	16-QAM
Proposed TTS-STBC	2.75 dB	5.30 dB
GSTBC [12]	3.54 dB	6.10 dB

TTS-STBC, three-time-slot space-time block code; GSTBC, group-decodable space time block code; QAM, quadrature amplitude modulation.
Note: Peak-to-average power ratio of a space time block code is calculated based on [13, Equation (3)].

When this paper is submitted, to my best acknowledge, the three-time-slot STBC for two transmit antennas are only in three references [4, 5] and [12]. Comparing the proposed STBC with STBCs in [4] and [5] is performed in subsection 6.2. Comparison results demonstrated that the proposed STBC outperforms STBC in [4] and [5]. For three-time-slot group-decodable STBC (named as GSTBC in this paper) in [12], its codeword matrix is given as

$$S_{GSTBC} = \begin{bmatrix} s_{1I} + s_{1Q} + js_{2I} + js_{2Q} & s_3 \\ -s_3^* & s_{1I} + s_{1Q} - js_{2I} - js_{2Q} \\ -s_{1I} + s_{1Q} - js_{2I} + js_{2Q} & -s_{1I} + s_{1Q} - js_{2I} + js_{2Q} \end{bmatrix} \quad (64)$$

relative motion between the transmitter and the receiver. In simulations, we consider a severely time-varying fading with $\psi = 0.9911$, which is a reasonable value in a mobile broadband system [7].

From Figure 5, we can see that the L-QOSTBC code [5] with the PML decoder suffer from serious error floor in the high-SNR regime. However, the proposed TTS-STBC code with SQML decoder allows an overcoming effect of time-varying fading. For example, it is observed that a roughly 5 dB SNR gain is achieved by the proposed TTS-STBC code over the L-QOSTBC code at a target symbol error rate (SER) of 2×10^{-3} without showing an error floor in the high-SNR regime. Therefore, we can also conclude that the proposed TTS-STBC code is more robust against the time-selectivity of fading channels by using a low complexity SQML decoder.

7. RELATED WORKS AND DISCUSSIONS

The proposed STBC is based on coordinate interleaved designs; it, however, is different from conventional coordinate interleaved designs in [10] and [11]. Firstly, the proposed STBC is designed specially for an even number of time slot (i.e. three time slots), while the coordinate interleaved designs in [10] and [11] are designed for odd number of time slot (e.g. 2, 4, 8, ... time slots). Secondly, all information symbol of codeword matrices in [10, 11] is coordinate interleaved, but it is not in the proposed STBC (e.g. u_2 in Equation (30)).

where $s_1, s_2, s_3 \in \mathrm{A}\,e^{\mathbf{j}0.0781\pi}$ and A is 4-QAM constellation. Simulation results in Figures 6 and 7 demonstrated that the proposed TTS-STBC outperforms than the GSTBC under time-selective fading channel, while they have the same performance under quasi-static fading channel.

In addition, the peak-to-average power ratio (PAPR) of the proposed STBC is 0.8 dB lower than that of the GSTBC [12] as shown in Table IV. The PAPR is an important property of an STBC. High PAPR requires a power amplifier with high power consumption and a large back off; such as an amplifier that is inefficient, bulky and expensive.

8. CONCLUSIONS

In this paper, we focus on designing STBC code for the LTE-advanced systems where Alamouti code is not fully supportive due to the fact that the number of time slots in an LTE-advanced frame is not always an even number. We proposed a TTS-STBC code for three-slot transmission. The proposed TTS-STBC code has some desirable properties such as full rate, full diversity, high coding gain and low decoding complexity. We also developed a low complexity SQML decoder for the proposed TTS-STBC code when fading is time-selective. Simulation results demonstrated that the proposed TTS-STBC code outperforms the reported 3-slot transmissions as the H-STBC code [4], L-QOSTBC code [5] and GSTBC [12]. Moreover, the proposed TTS-STBC code (with the SQML decoder) is more robust against the time-selectivity of fading channels. With these advantages, we believe that the proposed TTS-STBC code can become a prospective candidate for LTE-advanced uplink systems.

ACKNOWLEDGEMENTS

This work was partially supported under 322 Project granted by the Ministry of Education and Training of Vietnam. An author would like to thank Professor Sheng Wei Xing at the Nanjing University of Science and Technology, P. R. China for his valuable helps for this work.

REFERENCES

1. The 3rd Generation Partnership Project; Technical Specification Group Radio Access Network; Evolved Universal Terrestrial Radio Access (EUTRA); Physical Channels and Modulation (Release 8), 3GPP TS36.211 V8.3.0, (2008-05).
2. Alcatel Shanghai Bell, Alcatel-Lucent. STBC-II scheme for uplink transmit diversity in LTE-Advanced. R1-082500, 3GPP TSG RAN WG 1 Meeting #53 bis, Jun-Jul. 2008.
3. Alamouti SM. A simple transmit diversity technique for wireless communication. *IEEE Journal on Selected Areas in Communications* 1998; **16**(8): 1451–1458. DOI: 10.1109/49.730453.
4. Alcatel Shanghai Bell, Alcatel-Lucent, STBC-II scheme with non-paired symbols for LTE-Advanced uplink transmit diversity, R1-090058, 3GPP TSG RAN WG 1 Meeting #55 bis, Jan. 2009.
5. Lei ZD, Yuen C, Chin F. Quasi-orthogonal space-time block codes for two transmit antennas and three time slots. *IEEE Transactions on Wireless Communication* 2011; **10**(6): 1983–1991. DOI: 10.1109/TWC.2011.032411.101636.
6. Tran TA, Sesay AB. A generalized linear quasi-ML decoder of OSTBCs for wireless communications over time-selective fading channels. *IEEE Transactions on Wireless Communications* 2004; **3**(3): 855–864. DOI: 10.1109/TWC.2004.826326.
7. Lee HJ, Andrews JG, Powers EJ. Full rate STBCs from coordinate interleaved orthogonal designs in time-selective fading channels. *IEICE Transactions on Communications* 2008; **E91-B**(4): 1185–1189. DOI: 10.1093/ietcom/e91-b.4.1185.
8. Van Bien P, WeiXing S, Xuan Nam T, The Cuong D. Full-rate full-diversity three-time-slot space-time block code with single-symbol ML decoding, In *The 2011 International Conference on Advanced Technologies for Communications*, Hanoi, Vietnam, 2011; 207–211, DOI: 10.1109/ATC.2011.6027468.
9. Lee H, Cho J, Kim J, Lee I. An efficient decoding algorithm for STBC with multi-dimensional rotated constellations. *IEEE International Conference on Communications* 2006; **12**: 5558–5563. DOI: 10.1109/ICC.2006.255547.
10. Yuen C, Guan YL, Tjhung TT. Quasi-orthogonal STBC with minimum decoding complexity. *IEEE Transactions on Wireless Communications* 2005; **4**(5): 2089–2094. DOI: 10.1109/TWC.2005.853890.
11. Khan MZA, Rajan BS. Single-symbol maximum-likelihood decodable linear STBCs. *IEEE Transactions on Information Theory* 2006; **52**(5): 2062–2091. DOI: 10.1109/TIT.2006.872970.
12. Ren TP, Yuen C, Guan YL, Wang KH. 3-time-slot group-decodable STBC with full rate and full diversity. *IEEE Communication Letters* 2012; **6**(1): 86–88. DOI: 10.1109/LCOMM.2011.110711.111783.
13. Dayal P, Varanasi MK. Maximal diversity algebraic space-time codes with low peak-to-mean power ratio. *IEEE Transactions on Information Theory* 2005; **51**(5): 1691–1708. DOI: 10.1109/TIT.2005.846398.